Earth and Planetary Science Letters xxx (2011) xxx–xxx

Contents lists available at ScienceDirect

Earth and Planetary Science Letters

journal homepage: www.elsevier.com/locate/epsl

Thermo-mechanical reactivation of locked crystal mushes: Melting-induced internal fracturing and assimilation processes in magmas

Christian Huber [a,*], Olivier Bachmann [b], Josef Dufek [a]

[a] School of Earth and Atmospheric Sciences, Georgia Institute of Technology, Atlanta, United States
[b] Department of Earth and Space Sciences, University of Washington, Seattle, United States

ARTICLE INFO

Article history:
Received 5 September 2010
Received in revised form 11 February 2011
Accepted 14 February 2011
Available online xxxx

Editor: R.W. Carlson

Keywords:
magma chamber
mush
melting
crystallinity
fracturing
assimilation

ABSTRACT

Thermal reactivation of locked crystal mushes in the upper crust is a fundamental step towards volcanic eruptions of crystal-rich magmas. Models of such reactivation events indicate that partial melting of the crystalline framework is energetically costly and lead to average crystallinities that are lower than those observed in many erupted crystal mushes. Here, we show that internal overpressurization of the mush induced by small amounts of melting (10–20%) breaks the crystalline framework by microfracturing and allows for efficient unlocking of the mush. Hence, this melting-induced overpressurization, enhanced by addition of gas in wet magmatic systems, plays an important role in generating volcanic deposits with crystal contents close to the rheological lock-up (~50 vol% crystals) by accelerating the incorporation of highly crystalline parts of the magma chamber (self-assimilation). It can also participate in disintegrating pieces of country rock that are commonly scavenged in magmas, leading to bulk assimilation of crustal lithologies in shallow reservoirs.

1. Introduction

Crystal-rich volcanic deposits with obvious textural and geochemical evidence for pre-eruptive reheating imply that thermal reactivation is an important process in triggering the eruptions of shallow crustal magma reservoirs. The observed resorption textures and/or significant chemical zoning displayed by multiple mineral phases in a number of deposits are commonly interpreted as the result of a reheating event and unlocking of a crystal mush associated with the underplating intrusions of more mafic magma (Bachmann et al., 2002; Bachmann et al., 2007; Couch et al., 2001; Koyaguchi and Kaneko, 2001; Snyder, 2000). Some of the largest silicic eruptions preserved in the rock record, the Monotonous Intermediates (large dacitic ignimbrites with homogeneous whole-rock compositions); (Hildreth, 1981), provide formidable examples of such reactivated crystal mushes.

The main hypothesis for the reactivation of crystal-rich reservoirs (i.e. their transition from rheologically locked-up to sluggishly convecting magma body), is partial melting of the mineral assemblage associated with the emplacement of new magma intrusion at or near the base of the mush (e.g. (Bachmann et al., 2002; Bachmann et al., 2007; Couch et al., 2001; Murphy et al., 2000; Nakamura, 1995; Pallister et al., 1992)). Substantial amounts of enthalpy are required for the reactivation (Huber et al., 2010a; Huber et al., 2010b), and, for large systems, a single recharge event is generally not sufficient (the mafic intrusion has to be comparable in size with the mush). Moreover, the inefficient transfer of enthalpy between the intrusion and the mush fraction subjected to partial melting makes this process energetically unfavorable (Dufek and Bergantz, 2005; Huber et al., 2010b). (Huber et al., 2010b) also showed that the typical average crystallinities of erupted mushes are higher than expected from simple thermal models (i.e. melting models tend to overestimate the amount of melting required to reactivate a crystal mush), as conduction and convection models predict a large crystallinity reduction in the lowermost part of the mush when the melting/reactivation front reaches the top of the magma body. Therefore, we hypothesize that energy provided by the intrusion is not uniquely thermal. Exsolved volatiles injected by the intrusion and the volume change associated with the solid-melt phase transition in the mush can both provide some potential mechanical energy (overpressure).

In this study, we use a 1D multiphase thermal model coupled to a mechanical model to test the effect of the in-situ overpressurization associated with melting and the injection of volatiles on the reactivation of crystal mushes. As the reactivated part of the mush reaches a critical melting-induced overpressure (between 10^6 and 10^7 Pa; set here as 10^7 Pa; (Rubin, 1998)), the overlying mush is subjected to internal fracturing, the extent of which depends on the efficiency of the fracturing event to relieve the excess pressure. The style of fracturing is expected to

* Corresponding author.
E-mail address: christian.huber@eas.gatech.edu (C. Huber).

0012-821X/$ – see front matter © 2011 Elsevier B.V. All rights reserved.
doi:10.1016/j.epsl.2011.02.022

be a large number of microfractures rather than dikes, as (1) the stress state at the scale sampled by large dikes is overall compressive (due mostly to melting) and (2) the presence of a low viscosity compressible phase (exsolved volatiles) decreases the efficiency of the stress transmitted to the fracture tip. These fracturing episodes are expected to loosen up a small volume fraction of the overlying locked-up mush and, consequently, increase the volume of magma opened up to wholesale convection. The main advantages of these fracturing episodes are (1) it increases the energy efficiency required to reactivate crystal mushes, as melting provides most of the overpressure, and (2) it increases the average crystallinity of the these systems once reactivated. Both are required to better fit natural observations (Huber et al., 2010b).

This mechanical process of fracturing associated with melting applies to mush reactivation as a self-assimilation process ("defrosting" the overlying locked mush, observed both in volcanic; e.g., (Bachmann et al., 2002; Couch et al., 2001; Mahood, 1990) and plutonic sequences; e.g., (Paterson and Janousek, 2008; Robinson and Miller, 1999; Wiebe et al., 2007)), but can also play a role in assimilating country rocks in the case of magma evolution by AFC (Assimilation Fractional Crystallization; numerous papers, but see e.g., (Bowen, 1928; Daly, 1933; DePaolo, 1981; Taylor, 1980)). As blocks of crystalline wall rocks are incorporated into hot magmas, the mechanism of melting-driven fracturing will lead to enhanced disaggregation, allowing for rapid dissemination of small xenoliths and xenocrysts in the magma.

In the next section, we present the physical model used in this paper, describing shortly the thermal model (based on (Huber et al., 2010a)) and introducing the mechanical model (based and modified from (Huppert and Woods, 2002)). We also discuss the expected fracturing mechanism of the mush (large number of microcracks rather than one or a few large dikes) once a critical overpressure is reached. Finally, we present results from our numerical calculations and discuss the implications in the scope of the reactivation of large crystal-rich magma bodies.

2. Physical model

This section describes the model used to solve for the thermal and mechanical evolution of a silicic crystalline mush underplated by an intrusion of more mafic magma. We start by discussing the multiphase heat transfer between the intrusion and the mush and proceed next to a simple mechanical model based on mass conservation and linear elasticity to describe the evolution of the pressure during the reactivation of the mush.

2.1. Thermal model

The thermal model is similar to (Huber et al., 2010a) (illustrated schematically in Fig. 1). For simplicity, the intrusion is emplaced at once and the volume ratio between the mush and the intrusion is a free parameter in our calculations. The composition of the intrusion is set to andesitic and the mush to dacitic. The mush is assumed to be initially saturated with volatiles and we neglect volatile dissolution or exsolution associated with reheating and partial melting of the mush. We also assume that, by the time the intrusion reaches its emplacement depth (2×10^8 Pa), its volatile fraction mostly consists of water as a large fraction of the CO_2 already degassed and escaped towards the surface. The rate of cooling, crystallization and volatile exsolution in the intrusion is controlled by the heat transfer in the mush.

2.1.1. Underplating magma

We use a simplified relationship to describe the heat balance for the underplating intrusion

$$\frac{dT}{dt} = \underbrace{-\frac{q_{out}}{c_i\rho_i H_i}}_{\text{sensible heat}} + \underbrace{\frac{L_i}{c_i}\frac{\partial\chi_i}{\partial t}}_{\text{latent heat}}, \tag{1}$$

where the subscript i refers to the intrusion, H_i, L_i, c_i, ρ_i and χ_i are respectively the thickness, the latent heat of crystallization, the specific heat, the density and the crystallinity of the underplating magma body. q_{out} is the heat transfer from the intrusion to the mush and therefore couples the magma body in terms of heat transfer. This heat balance equation assumes a well-mixed intruding magma with negligible thermal gradients which is a relatively good approximation when a fluid body with strong temperature dependent viscosity convects. We use stagnant-lid convection scalings to calculate the convective heat flux out of the intrusion using a temperature and crystallinity-dependent viscosity (Huber et al., 2010a). The crystallinity–temperature relationship for an andesitic intrusion (likely composition for recharge in continental arcs) is calculated with MELTS (Ghiorso and Sack, 1995) using the major element composition listed in (Parat et al., 2008) for the Huerto andesite (San Juan Volcanic Field, Colorado). We assume an initial water content of 6 wt.% H_2O. We also use MELTS to parameterize the exsolution of volatiles (water only in this case, see section below) as function of temperature (see (Huber et al., 2010a)).

We assume that the transport of exsolved volatiles from the intrusion to the mush can be described by a multiphase Darcy equation

$$q_{H_2O} = \frac{kk_r\Delta\rho g}{\mu_g}, \tag{2}$$

where k and k_r are the permeability of the magma and the relative permeability for the volatile phase, respectively, $\Delta\rho$ is the density contrast between the melt and the volatile phase and g is the acceleration due to gravity. The permeability is related to the crystallinity by the Carman–Kozeny relation (Bear, 1988)

$$k = A\frac{(1-\chi_i)^3}{(1-(1-\chi_i))^2}, \tag{3}$$

where the constant A is set to 2×10^{-12} m^2, leading to a permeability $k=10^{-12}$ m^2 at $\chi_i=0.5$. Many empirical and theoretical expressions have been derived for the dependence of the relative permeability on the volatile volume fraction, we use the following expression

$$k_r\left(S_g\right) = S_g^4, \tag{4}$$

where S_g is the volume fraction of exsolved volatiles. For a more detailed description of the volatile transport model, the reader is referred to (Huber et al., 2010a).

2.1.2. Crystal mush

The mush above the intrusion has initially a crystallinity ranging from 51 to 67%. We solve for the mass conservation of volatiles (initially exsolved from the intrusion)

$$\frac{\partial\left(\rho_g(1-\chi_{\text{mush}})S_g\right)}{\partial t} = -\frac{\partial\left(\rho_g u_{d,z}\right)}{\partial z}, \tag{5}$$

where $\rho_g=\rho_{H_2O}$, χ_{mush} is the crystallinity of the mush, S_g is the pore volume fraction occupied by the volatiles and $u_{d,z}$ is the z-component of the Darcy velocity for the volatile phase and z is parallel to gravity (increases upwards). The boundary condition at the interface between the mush and the intrusion requires matching the volatile flux (see Eq. (2)). We assume here that the melt is volatile-saturated and that no further degassing or dissolution of volatiles occurs within the mush. The flux of volatiles is obtained from a multiphase Darcy equation

$$u_{d,z} = -\frac{k_{\text{mush}}k_{\text{rmush}}}{\mu_{H_2O}}\frac{\partial}{\partial z}\left[\left(\rho_{H_2O}(z)-\rho_{\text{melt}}\right)gz\right] \tag{6}$$

Please cite this article as: Huber, C., et al., Thermo-mechanical reactivation of locked crystal mushes: Melting-induced internal fracturing and assimilation processes in magmas, Earth Planet. Sci. Lett. (2011), doi:10.1016/j.epsl.2011.02.022

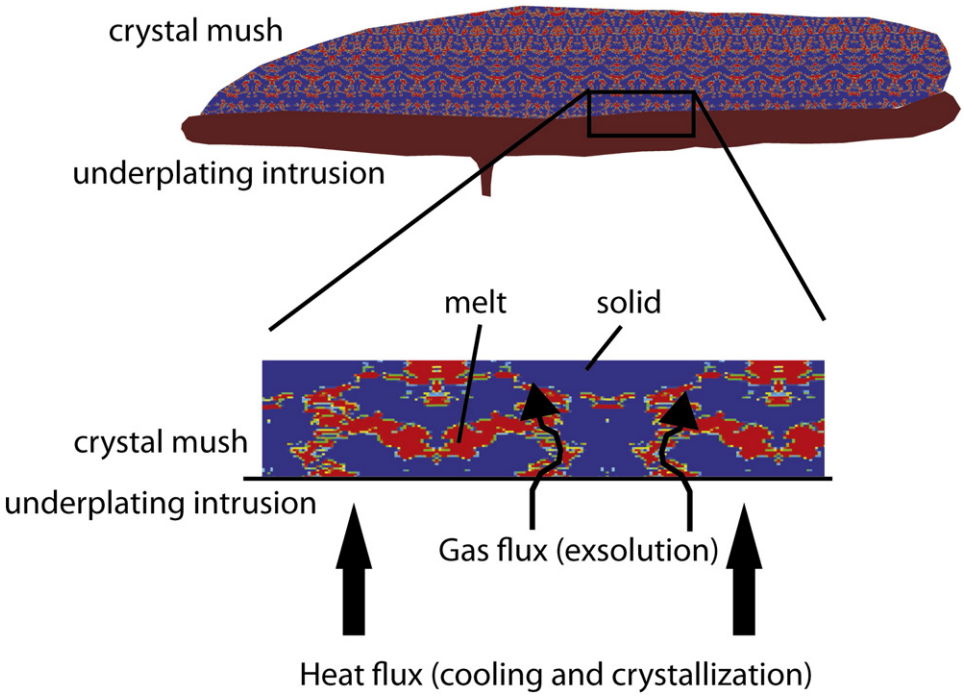

Fig. 1. Schematic representation of the coupled mush–intrusion system. The two magmas exchange heat and the mush is subjected to injections of volatiles exsolved from the underlying intrusion (Huber et al., 2010a, 2010b).

where g is the acceleration due to gravity and is counted positive upwards, k_{mush} and k_{rmush} are respectively the permeability and relative permeability of the mush for the volatile phase. Finally, μ_{H_2O} is the dynamic viscosity of the volatile phase which, for simplicity, was fixed here to 10^{-5} Pa s (Assael et al., 2000). For more details on the treatment of the multiphase permeability, the reader is referred to (Huber et al., 2010a).

We assume a simple power-law for the crystallinity–temperature relationship that captures the main features of calc-alkaline dacitic magmas (Huber et al., 2010a; Huber et al., 2010b). The crystallinity in the mush is given by

$$\chi_{\mathrm{mush}} = 1-\left(\frac{T-T_{sol}}{T_{liq}-T_{sol}}\right)^{0.5}, \tag{7}$$

T_{sol}, T_{liq} are the solidus and liquidus temperatures, respectively set to 700 and 950 °C.

The melting of the mush is obtained by solving the energy balance that includes heat diffusion, absorption of latent heat during the partial melting of the mush and advection of heat by the volatile phase,

$$\frac{\partial(\rho_{\mathrm{mix}}c_{\mathrm{mix}}T)}{\partial t} = -\frac{\partial}{\partial z}\left(c_g\rho_{H_2O}u_{d,z}T\right) + \frac{\partial}{\partial z}\left(k_{\mathrm{mix}}\frac{\partial T}{\partial z}\right) + \rho_s L\frac{\partial \chi_{\mathrm{mush}}}{\partial t}. \tag{8}$$

In Eq. (8), the specific heat of the volatiles c_g is assumed constant (3880 J/kg K) (Lemmon et al., 2003), ρ_{H_2O} is calculated with the Modified Redlich–Kwong equation of state (Halbach and Chatterjee, 1982; Huber et al., 2010a), and ρ_s is the average density of the crystalline phase subjected to melting. Eq. (8) assumes that the volatile phase is locally in thermal equilibrium with the melt and crystals, which assumes a low Peclet number (i.e. $\mathrm{Pe} = u_{d,z}R/\kappa < 1$, R is the average pore radius and κ the average thermal diffusivity) which is found to be consistent with our numerical results. The density, specific heat and thermal conductivity of the solid–melt–volatiles mixture are calculated with

$$\rho_{\mathbf{mix}} = \rho_m(1-\chi_{\mathrm{mush}})\left(1-S_g\right) + \rho_s\chi_{\mathrm{mush}} + \rho_{H_2O}(1-\chi_{\mathrm{mush}})S_g \tag{9}$$

$$c_{\mathbf{mix}} = \frac{\rho_m(1-\chi_{\mathrm{mush}})\left(1-S_g\right)c_m + \rho_s\chi_{\mathrm{mush}}c_s + \rho_{H_2O}(1-\chi_{\mathrm{mush}})S_gc_g}{\rho_m(1-\chi_{\mathrm{mush}})\left(1-S_g\right) + \rho_s\chi_{\mathrm{mush}} + \rho_{H_2O}(1-\chi_{\mathrm{mush}})S_g} \tag{10}$$

$$k_{\mathbf{mix}} = \frac{1}{2}\left\{\left(\frac{(1-\chi)S_g}{2k_g+k_g} + \frac{(1-\chi)\left(1-S_g\right)}{2k_g+k_m} + \frac{\chi}{2k_g+k_s}\right)^{-1} - 2k_g \right. \tag{11}$$

$$\left. + \left(\frac{(1-\chi)S_g}{2k_s+k_g} + \frac{(1-\chi)\left(1-S_g\right)}{2k_s+k_m} + \frac{\chi}{2k_s+k_s}\right)^{-1} - 2k_s\right\} \tag{12}$$

where the subscript s,m,g refer to solid, melt and volatiles respectively. The mixture thermal conductivity is obtained using the Hashin–Shtrikman–Walpole bounds (Hashin and Shtrikman, 1963; Torquato, 2001). Table 1 lists the different parameters used in the physical model.

2.2. Mechanical model

In the following section we derive the equations for the evolution of pressure from mass conservation. We separate the treatment for the part of the mush opened to convection (where the crystallinity is lower than 0.45) from the part of the mush still rheologically locked overlying it.

2.2.1. Reactivated part of the mush

We use an analogous treatment as in (Huppert and Woods, 2002). From mass conservation, the opened part of the mush of volume

Please cite this article as: Huber, C., et al., Thermo-mechanical reactivation of locked crystal mushes: Melting-induced internal fracturing and assimilation processes in magmas, Earth Planet. Sci. Lett. (2011), doi:10.1016/j.epsl.2011.02.022

Table 1
List of parameters and symbols.

Symbol	Description	Value	Units
c_x	Specific heat for phase x		J/kg/K
g	Acceleration due to gravity		m^2
H	Mush thickness	2000	m
k_{cond}	Thermal conductivity at intrusion–mush interface	2	W/m/K
k_g, k_s, k_m	Thermal conductivity of volatile, crystals and melt	0.31, 1.4, and 2	W/m/K
k/k_r	Permeability and relative permeability (mush or intrusion)		m^2
L_i/L	Latent heat of crystallization (intrusion/mush)	270	kJ/kg
S	Surface area of contact between intrusion and mush	2×10^8	m^2
S_g	pore volume fraction occupied by volatiles		
T_{ini}	Initial temperature of intrusion	850	°C
$u_{d,z}$	Vertical component of Darcy velocity for volatile phase (mush)		m/s
V_r	Volume of ratio intrusion to mush	0.1, 0.25, 0.33, 0.5 and 1	
α	Expansion coefficient (thermal and crystallinity)	3×10^{-5}	1/T
β_i	Bulk modulus of phase i		Pa
$\chi_i/\chi_{\text{mush}}$	Crystallinity of intrusion/mush		
χ_{cr}	Critical crystallinity	0.45	
κ	Thermal diffusivity	10^{-6}	m^2/s
ρ_x	Density of a given phase		kg/m^3
μ_x	Dynamic viscosity of a given phase		Pa s

$V = S\times H$, where S is the surface area and H the thickness of the part of the mush that melted to a crystallinity lower than 0.45, obeys

$$\frac{d\overline{\rho}V}{dt} = \overline{\rho}\frac{dV}{dt} + V\frac{d\overline{\rho}}{dt} = Q - J_p S\overline{\rho}. \tag{13}$$

Here $\overline{\rho}$ is the multiphase density averaged over the volume of the reactivated part of the mush

$$\overline{\rho} = \frac{1}{V}\int_V \Big(\rho_s(1-\phi(\mathbf{x},t)) + \rho_m\phi(\mathbf{x},t)\Big(1-S_g(\mathbf{x},t)\Big) + \rho_g(\mathbf{x},t)\phi(\mathbf{x},t)S_g(\mathbf{x},t)\Big)dV, \tag{14}$$

where the subscripts s, m and g refer respectively to crystals, silicate melt and exsolved volatiles, ϕ is the local porosity in the reactivated volume and S_g the local volatile pore volume fraction. In Eq. (13), Q represents the source of mass associated with the injection of volatiles from the underlying intrusion and J_p represents the flux out term

$$J_p = -\frac{k}{\mu^{(2)}_{HS}}\frac{\partial p}{\partial z}|_{up}, \tag{15}$$

with k and $\mu^{(2)}_{HS}$ being the average permeability and two-phase viscosity (silicate melt and volatiles) at the interface between the mush and its reactivated part. These parameters will be defined in the next section. The volume change term of Eq. (13) accounts for the volume change associated with pressure changes

$$\frac{dV}{dt} = \frac{V}{\beta_r}\frac{dp}{dt}, \tag{16}$$

where β_r is the average bulk modulus of the rocks surrounding the reactivated part of the mush (which takes into account also the stiff mush above it). Using the chain rule to expand the variation of average density with time in terms of porosity and pressure changes

$$\frac{d\overline{\rho}}{dt} = \frac{\partial\overline{\rho}}{\partial p}\frac{dp}{dt} - \Delta\rho\frac{d\overline{\phi}}{dt} = \frac{\overline{\rho}}{\beta^{(3)}_{HS}}\frac{dp}{dt} - \Delta\rho\frac{d\overline{\phi}}{dt}, \tag{17}$$

where $\Delta\rho = \rho_s - \rho_m$ and $\beta^{(3)}_{HS}$ is the multiphase average bulk modulus obtained with the Hashin–Shtrikman–Walpole bounds (the superscript refers to the number of phases involved, crystals, melt and volatiles) (Hashin and Shtrikman, 1963; Torquato, 2001).

$$\beta^{(3)}_{HS} = \frac{1}{2}\left(\frac{(1-\overline{\phi})}{\beta_s + \frac{4}{3}G_{min}} + \frac{\overline{\phi}\,\overline{S}_g}{\beta_g + \frac{4}{3}G_{min}} + \frac{\overline{\phi}\left(1-\overline{S}_g\right)}{\beta_m + \frac{4}{3}G_{min}}\right)^{-1} - \frac{4}{3}G_{min} + \left(\frac{(1-\overline{\phi})}{\beta_s + \frac{4}{3}G_{max}} + \frac{\overline{\phi}\,\overline{S}_g}{\beta_g + \frac{4}{3}G_{max}} + \frac{\overline{\phi}\left(1-\overline{S}_g\right)}{\beta_m + \frac{4}{3}G_{max}}\right)^{-1} + \frac{4}{3}G_{max}\}, \tag{18}$$

where $\bar{a}$ is understood as a volumetric average of variable a taken over the reactivated part of the mush (see Eq. 14). $G_{\min}$ and $G_{\max}$ are respectively the minimum and maximum shear modulus taken over the three phases (respectively 0 and about 4×10^{10} Pa). Rearranging the different terms of Eq. (13) we obtain

$$\frac{dp}{dt} = \left(\frac{1}{\beta_r} + \frac{1}{\beta^{(3)}_{HS}}\right)^{-1}\frac{\left(Q + \Delta\rho\frac{d\overline{\phi}}{dt}V - J_p A\overline{\rho}\right)}{\overline{\rho}V} \tag{19}$$

Our simple model does not account for viscoelastic effects such has viscous relaxation of the surrounding crust. These effects are tested by running the calculations for two end-member choices of host-rock bulk modulus.

2.2.2. Mush

The part of the mush with a crystallinity above 0.45 is treated separately as the solid fraction modifies its rheological behavior and the crystal fraction forms a rigid framework. The local mass conservation equation becomes

$$\frac{d(\phi\overline{\rho})}{dt} = \overline{\rho}\frac{d\phi}{dt}|_T + \phi\frac{d\overline{\rho}}{dt} = -\frac{\partial\overline{\rho}u_z}{\partial z} + \Delta\rho\frac{d\phi}{dt}|_p, \tag{20}$$

where $\overline{\rho}$ is now the local two phase volume-averaged density (silicate melt and volatiles), u_z is the multiphase fluid mixture vertical velocity, $\frac{d\phi}{dt}|_T$ and $\frac{d\phi}{dt}|_p$ are respectively the pore volume changes associated with pressure (fixed temperature) and with melting (fixed pressure).

Please cite this article as: Huber, C., et al., Thermo-mechanical reactivation of locked crystal mushes: Melting-induced internal fracturing and assimilation processes in magmas, Earth Planet. Sci. Lett. (2011), doi:10.1016/j.epsl.2011.02.022

Recasting density variations in terms of pressure variations (recognizing here that the melting term is already accounted for in $\frac{d\phi}{dt}|_p$), we get

$$\frac{d\phi}{dt}|_T = \frac{1}{\beta_{matrix}}\frac{dp}{dt}, \tag{21}$$

where β_{matrix} is the bulk modulus of the solid matrix. Using Darcy's equation for u_z, we obtain

$$\frac{dp}{dt} = \left(\frac{1}{\beta_{matrix}} + \frac{\phi}{\beta_{HS}^{(2)}}\right)^{-1}\left\{-\frac{1}{\overline{\rho}}\frac{\partial}{\partial z}\left[-\frac{\overline{\rho}k}{\mu_{HS}^{(2)}}\frac{\partial p}{\partial z}\right] + \frac{\Delta o}{\overline{\rho}}\frac{d\phi}{dt}|_p\right\}. \tag{22}$$

The local averages $\beta_{HS}^{(2)}$ and $\mu_{HS}^{(2)}$ are calculated with

$$\beta_{HS}^{(2)} = \left(\frac{S_g}{\beta_g} + \frac{\left(1-S_g\right)}{\beta_m}\right)^{-1}, \tag{23}$$

and

$$\mu_{HS}^{(2)} = \frac{1}{2}\left\{\left(\frac{S_g}{\mu_g + \frac{2}{3}\mu_g} + \frac{\left(1-S_g\right)}{\mu_m + \frac{2}{3}\mu_g}\right)^{-1} - \frac{2}{3}\mu_g + \left(\frac{S_g}{\mu_g + \frac{2}{3}\mu_m} + \frac{\left(1-S_g\right)}{\mu_m + \frac{2}{3}\mu_m}\right)^{-1} - \frac{2}{3}\mu_m\right\}, \tag{24}$$

where μ_g and μ_m are respectively the dynamic viscosities of the volatile and silicate melt phases. We note that these properties depend on two phases (melt and gas) instead of three as in the reactivated part of the mush, because crystals here are no longer assumed to be part of the suspension, but form a rigid framework. The effect of the solid fraction on the pressure field (compaction for example) is incorporated into the term β_{matrix} of Eq. (22). Similarly the resistance to the flow of melt and gas is not accounted for in the multiphase viscosity as for the reactivated part, but is introduced by the permeability in Eq. (22). The mechanical and thermal models are coupled by the equation of state for the volatile phase (here using a modified Redlich–Kwong relationship, (Huber et al., 2010a)) that relates the pressure and temperature in the volatile phase to its density which in turns affect the volatile saturation S_g. The mechanical, thermal and transport properties in the mush are strongly controlled by the volatile phase saturation.

2.3. Fracturing versus diking

The pressure in the mush increases during the reactivation because of two effects (the first two terms of the right-hand side of Eq. (19)). First, the injection of volatiles from the intrusion increases the overall mass contained in the mush system. Due to the difference of density between the volatile phase and the other constituents of the magma and its greater compressibility, this effect remains relatively weak as long as the injection rate is not too elevated. Second, the density difference between the melt and crystals (about 10%) and the low compressibility of these two phases lead to an increase of pressure resulting from melting (average density of the magma decreases). The overpressure therefore builds up where the melting is the most intense, near the mush opening front. The overpressure is assumed to be mostly homogeneous in the reactivated part of the mush, however, in the locked-up part, the pore pressure diffuses upward from the reactivated part along the hydraulic gradient. The multiphase hydraulic diffusivity of the mush (which depends on the permeability of the mush, the viscosity of the magma mixture and the effective compressibility of the mush–host rock system) is expected to reduce the build-up of overpressure in the reactivated part of the mush as well as the pressure gradient between the two parts of the mush.

We assume that the locked-up mush behaves as a brittle solid, which, as we will see below, is consistent with our numerical results, the period between fracturing episodes being usually much shorter than the viscous relaxation timescale for the mush ($>10^8-10^{15}$ s, (Karlstrom et al., 2010)). We therefore expect that if the overpressure reaches a critical value, cracks will start to propagate. (Rubin, 1998) showed that the expected overpressure to propagate dikes in partially molten rocks is about 10^6 to 10^7 Pa. For a mush at a confining pressure of about 2 kb, the fracture threshold is only about 5% of the effective pressure in the mush and is therefore not too difficult to reach for a dynamical system with phase changes and injected with volatiles from a different magmatic source.

We assume that once a critical overpressure is reached, a fracturing event is triggered, reducing the pressure in the mush. A valid question subsists: once a fracture is initiated, does it grow to form a dike? We use two qualitative arguments that argue for another possible process than diking. Mid-size to large silicic mush have a large aspect ratio (greater width than thickness), consequently most of the overpressurized mush is not expected to be substantially influenced by the edges of the magma body. Fractures are expected to initiate at the weakest points bounding the reactivated mush. We assume that the part of the mush just above the reactivation front is the weakest as its crystallinity barely exceeds the locking point threshold. By definition, the mush at the contact with the reactivation front is at the rheological transition between a fluid and brittle solid. The initiation of cracks is expected to loosen up the weakest part of the mush before the fractures grow to form dikes. The strength of the lowermost part of the locked mush is expected to increase because of the sharp crystallinity gradients above the melting front, which would tend to deflect propagating cracks horizontally as they penetrate higher crystallinity environments. A possible scenario is the development and opening of microfractures at the contact between crystals oriented sub-parallel to the normal of the mush front (see Fig. 2 for an illustration). The increased pore-pressure is also expected to reduce the strength of the mush at the melting front. As the largest gradients of pressure are expected to be located at the front between the reactivated and locked-up mush, where volatiles are expected to be present, initiated cracks open and are expected to fill up more efficiently with volatiles owing to the slow response of the very viscous melt. The cracks should therefore contain a large fraction of volatiles which is much more compressible than melt or crystals. In our model, unlike (Menand and Tait, 2001), the opening of cracks is pressure-driven. The propagation of the overpressure at the crack tip is therefore expected to be less efficient than for a crack filled with an incompressible fluid.

In summary, we hypothesize that once the overpressure in the mush reaches a critical value, a microfracturing event is triggered, where a large number of closely spaced cracks are initiated. These cracks do not penetrate as deep in the mush as we would expect for a typical dike. The overpressure is relieved because of the high density of cracks that leads to the loss of strength of the lowermost part of the locked-up mush (see Fig. 2). A part of the mush is therefore assimilated mechanically into the reactivated part, the volume of which depends on the ability of this process to relieve overpressure. Another way to understand this process is to view the microfracturing event as a sink of overpressure in Eq. (19) associated with the sudden change of the average density of the magma in the reactivated part of the mush. The assimilation results in an increase of average crystallinity in the reactivated part and consequently an increase in density. The drop in pressure associated with the microfracturing event is given by

$$\Delta p = \beta_{\mathrm{eff}}\frac{\Delta\overline{\rho}}{\overline{\rho}}, \tag{25}$$

Please cite this article as: Huber, C., et al., Thermo-mechanical reactivation of locked crystal mushes: Melting-induced internal fracturing and assimilation processes in magmas, Earth Planet. Sci. Lett. (2011), doi:10.1016/j.epsl.2011.02.022

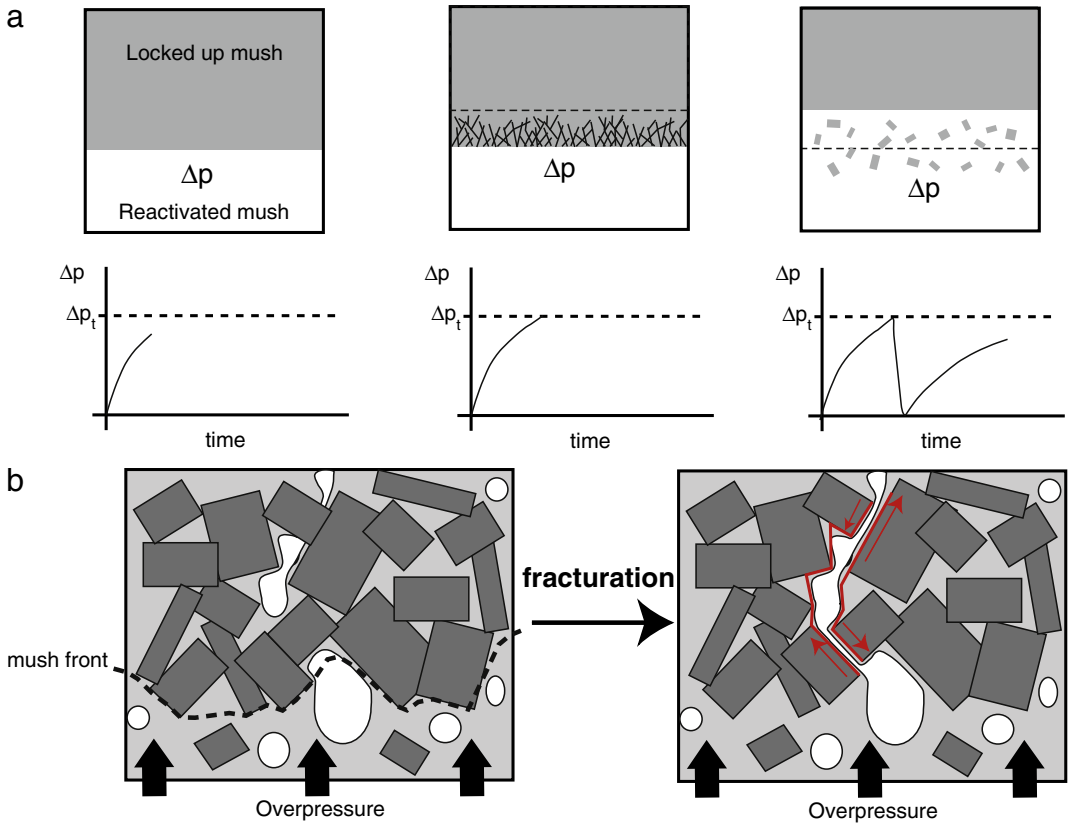

Fig. 2. Our conceptual mush fracturing model. The upper row illustrates the termporal evolution of the mush and the build-up of overpressure associated with melting. Once the overpressure reaches a critical value, the weakest part of the mush breaks and is assimilated by the reactivated part. The lowest row depicts schematically the fracturing process at the crystal-scale.

where β_{eff} is the effective bulk modulus

$$\beta_{\text{eff}} = \left(\frac{1}{\beta_r} + \frac{1}{\beta_{HS}^{(3)}}\right)^{-1}. \tag{26}$$

The difference in average magma density before and after the crack is

$$\Delta\overline{\rho} = \overline{\rho}_{\text{after}} - \overline{\rho}_{\text{before}} = \frac{\overline{\rho}_{\text{mush}}\Delta V_{\text{frac}} + \overline{\rho}_{\text{open}} V_{\text{open}}}{V_{\text{open}} + \Delta V_{\text{frac}}} - \overline{\rho}_{\text{open}}, \tag{27}$$

where $\overline{\rho}_{\text{mush}}$ is the average crystallinity of the mush just above the reactivation front, $\overline{\rho}_{\text{open}}$ is the average density in the reactivated part of the mush, V_{open} is the volume of mush reactivated before the fracturing episode and ΔV_{frac} is the volume of locked-up mush assimilated because of the fracturing event.

Using Eq. (25) together with Eq. (27), we can write

$$\Delta V_{\text{frac}} = \frac{\Delta p}{\beta_{\text{eff}}\left(\frac{\overline{\rho}_{\text{mush}}}{\overline{\rho}_{\text{open}}} - \left(1 + \frac{\Delta p}{\beta_{\text{eff}}}\right)\right)} V_{\text{open}}. \tag{28}$$

Assuming for simplicity that the average crystallinity and volatile saturation in the reactivated part of the mush are respectively 0.3 and 0.2, and using an average crystallinity of 0.5 for the mush just above the reactivated front (using the same volatile saturation), then $\overline{\rho}_{\text{mush}} / \overline{\rho}_{\text{open}} \simeq 5/4$, and Eq. (28) can be reduced approximately to

$$\Delta V_{\text{frac}} \simeq 4\frac{\Delta p}{\beta_{\text{eff}}} V_{\text{open}}. \tag{29}$$

In Eq. (29), Δp is assumed to be about 10^7 Pa (overpressure is fully relieved by fracturing).

This microfracturing process acts like a self-assimilation mechanism driven by the mechanical energy (overpressure) associated with the phase change during the reactivation of the mush. Once the fragments of the locked-up mush are assimilated in the convecting part of the mush, the energy efficient reactive assimilation processes described by (Beard et al., 2005) can reduce the size of the fragments from a size equivalent to the penetration depth of cracks (cm scale, see results) to the scale of crystals. As the assimilate mixes in a magma with the same composition, this process is petrologically transparent.

3. Numerical model

The thermal modeling is similar to (Huber et al., 2010a). The 1D energy and mass conservation equations, together with the constitutive equations for the crystallinity–temperature relationships, the permeability–porosity relationship and the multiphase permeability are solved iteratively at each timestep. Eqs. (19) and (22) are introduced in the iterative scheme for the mush evolution to calculate the overpressure evolution in the reactivated and locked-up part of the mush respectively.

As a result of the injection of volatiles from the intrusion and melting, the pressure in the mush increases (see Eq. (19)). We use a threshold value for the overpressure of $\Delta p = 100$ Pa beyond which a fraction of the locked-up mush is expected to experience brittle failure (fracturing). Each fracturing episode is expected to efficiently relieve the overpressure of the system (reset to 0). Our numerical model does not directly solve for the effect of fracturing on the evolution of the mush, but allows us to calculate the frequency of

Please cite this article as: Huber, C., et al., Thermo-mechanical reactivation of locked crystal mushes: Melting-induced internal fracturing and assimilation processes in magmas, Earth Planet. Sci. Lett. (2011), doi:10.1016/j.epsl.2011.02.022

fracturing episodes and estimate the volume of mush affected by the microcracks.

4. Results

We calculated the thermal and mechanical evolution of the mush for the first 1000 years after the emplacement of an andesitic intrusion. We assume a power–law relationship for the crystallinity–temperature relationship of the mush (power-law exponent of 0.5 in Eq. (7)) and a magma volume ratio (intrusion/mush) of 1/10, 1/4, 1/3, 1/2 and 1. The initial crystallinity of the mush was assumed to be 0.505, 0.55, 0.6, 0.65 and 0.67.

The results showing the temperature, pressure and volatile saturation (pore volume fraction) profiles obtained after a thousand years for an intrusion to mush volume ratio of 1/3, an initial mush crystallinity of 0.55 and assuming the bulk modulus of the host-rocks to be 10^{11} Pa are presented in Fig. 3. Fig. 3a shows that the heat transferred by the intrusion reached about 1/5 of the thickness of the mush, which is consistent with the porosity profile (melting) shown in Fig. 3b. The third panel, Fig. 3c, shows the volatile content which penetrated deeper into the mush than the heat associated with the intrusion. As discussed by (Huber et al., 2010a), the maximum volatile saturation observed is 0.2, consistent with the choice of critical saturation threshold where volatiles become much more mobile. The last panel (d) shows the overpressure in the mush. In the reactivated part of the mush, the overpressure is homogenous at 7×10^6 Pa. The penetration distance in the locked-up mush is controlled by the hydraulic diffusivity of the magma mixture in the locked-up mush. The overpressure does not penetrate deep into the locked-up mush because of the large viscosity of the magma and the moderate permeability of the mush (set up here to 10^{-12} m^2 at a crystallinity of 0.5).

The frequency of fracturing episodes can be deduced directly from the calculations. Each time the overpressure reaches the critical threshold corresponds to a fracturing event, after which the overpressure is reset to zero, before building up for the next event. Fig. 4a shows the period of fracturing events versus time for a mush with initial crystallinity of 0.55, with an intrusion to mush volume ratio of 1/3 and assuming a host-rock bulk modulus of 10^{11} Pa. The period increases with time according to power–law $\sim 0.036t^{1.12}$. Fig. 4b shows the position of the melting front coinciding with the transition from a rheologically locked mush to its reactivated part. The power–law we observe is consistent with the simplification made in the thermal model, where we assumed the heat transfer in the mush to be conductive except for the advective transfer associated with the rise of buoyant volatiles. The stepped nature of the results here is due to the spatial resolution limitation of the numerical model, reasonably good fits are however easy to obtain to get an average melting trend.

Fig. 5 shows that the relationship between the fracturing period and time depends strongly on the volume ratio of the two magmas V_r. The fracturing frequency is significantly higher for larger intrusions. The effect of the initial mush crystallinity (not shown here) is however much more tenuous.

Using the power–laws obtained by fitting the progress of the melting front and the evolution of the fracturing period with time together with Eq. (29), we can calculate the effect of fracturing events on the reactivation of crystal mushes. The evolution of the position of the melting front (Fig. 4b) allows us to estimate the growth of the reactivated fraction between fracturing episodes. The growth of the

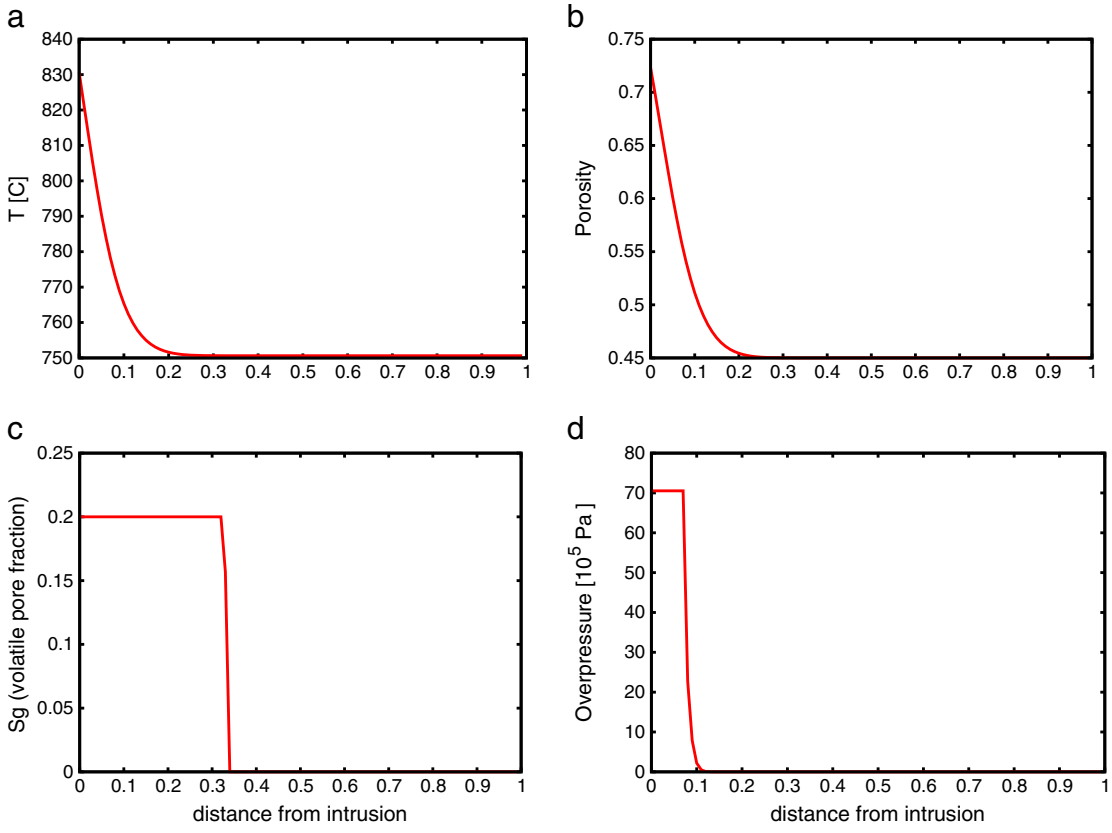

Fig. 3. Profiles of temperature (a), melt fraction (b), volatile saturation (c) and overpressure (d) with vertical distance from the mush–intrusion boundary. These profiles show the state of a mush with an initial crystallinity of 0.55, underplated by an intrusion with a volume three times smaller than the mush after 1000 years. The host rocks bulk modulus is set here to 10^{11} Pa.

Please cite this article as: Huber, C., et al., Thermo-mechanical reactivation of locked crystal mushes: Melting-induced internal fracturing and assimilation processes in magmas, Earth Planet. Sci. Lett. (2011), doi:10.1016/j.epsl.2011.02.022

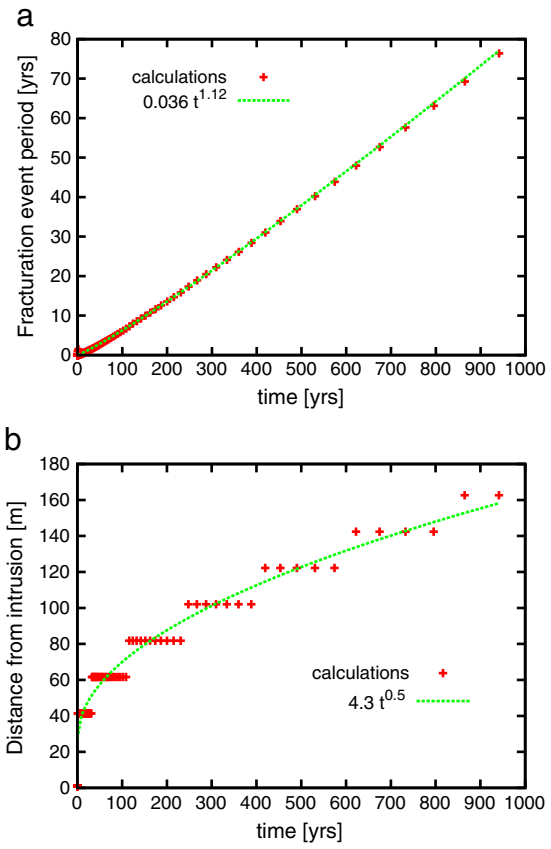

Fig. 4. (a) Period between fracturing episodes versus time (shown with a power–law fit) and (b) the propagation of the melting front with time (also with fit). The initial crystallinity of the mush is 0.55, the intrusion–mush volume ratio is 1/3 and the host-rock bulk modulus is 10^{11} Pa. The stepped nature of the melting front propagation results from the relatively low spatial resolution in the mush (see the text for more details).

reactivated portion of the mush can be obtained with the following iterative procedure

$$V_{\mathrm{open},n}(t)=\underbrace{\left(V_{\mathrm{open},n-1}(t-\mathcal{T}_{n-1})+\underbrace{\mathcal{A}\left(t^{\mathcal{B}}-(t-\mathcal{T}_{n-1})^{\mathcal{B}}\right)}_{\text{melting}}\right)}_{V\text{prior to fracturing n}}\left(1+4\frac{\Delta p}{\beta_{\mathrm{eff}}}\right), \tag{30}$$

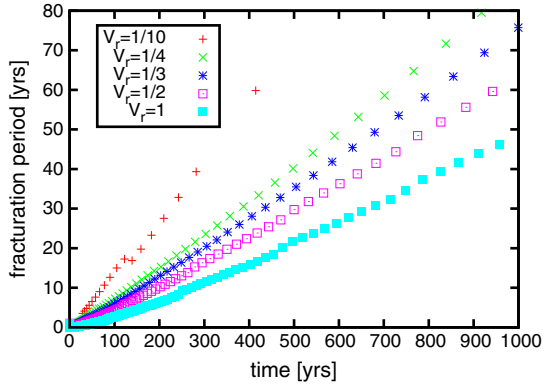

Fig. 5. Illustration of the dependence of the period between fracturing episodes on the intrusion–mush volume ratio V_r. These calculations are done for a mush with an initial crystallintiy of 0.6 and a host-rock bulk modulus of 10^{11} Pa.

where $V_{\mathrm{open},n}(t)$ is the volume of reactivated mush after the fracturing episode n at time t, $\mathcal{T}_{n-1}$ is the period between fracturing episode n and $n-1$, $\mathcal{A}$ and $\mathcal{B}$ are the two fitting constants obtained from the melting front propagation. The set of periods $\mathcal{T}_i(t)$ are also obtained by a fitting procedure (see Fig. 4a). Fig. 4 shows the effect of the fracturing process on the reactivation of a mush for a choice of $V_r=1/2$, a mush initial crystallinity of 0.67 and assuming that the bulk modulus of the host rocks is 10^{11} Pa. We quantify the efficiency of the self-assimilation process (fracturing) by computing the ratio of volume reactivated with and without fracturing episodes (see Fig. 6b)

$$\zeta(t)\equiv\frac{V_{\mathrm{open},n}(t)}{V_{\mathrm{melting}}(t)}. \tag{31}$$

We observe in general that the efficiency increases strongly at early times (values $\gg 1$) and decreases steadily afterwards although remaining substantially greater than 1. The last panel of Fig. 6(c) shows the depth over which each fracturing episode penetrates in the locked part of the mush. We see that the crack lengths are typically under the meter scale. Although the volume assimilated during each cracking episode is relatively small, the number of fracturing events is large owing to the low critical threshold for fracturing (10^7 Pa), especially shortly after the emplacement of the intrusion. These general features are common to all the calculations we conducted, Fig. 7 shows some of our calculations for (1) a constant magma volume ratio $V_r=1/3$ in the first two rows and (2) a constant crystallinity ($\chi=0.6$) for the last two. The dependence of the volume of mush reactivated on the initial crystallinity of the mush is complex because of the competition between two effects. The volume of mush reactivated by melting alone tends to be smaller for high initial crystallinity, as the propagation of the melting front is slower. The greater amount of melting required induces a higher frequency of fracturation episodes, however, each of these fracturation event leads to a smaller amount of assimilated mush from Eq. (28).

We calculated the fracturing efficiency $\zeta(t=1000$ years) for a range of initial mush crystallinity (0.51, 0.55, 0.6, 0.65 and 0.67) and a range of intrusion to mush volume ratio $V_r=1/10, 1/5, 1/3, 1/2$ and 1. Fig. 8 shows the efficiencies ζ for two different host-rock bulk modulus values, the first one (a) represents the case where host rocks remained rigid and the second (b) represents the other end-member when heat transfer and deformation during the emplacement of the intrusion made the host rocks much weaker. We arbitrarily chose an effective bulk modulus β_{eff} consistent with the choice of host-rock and multiphase magma bulk moduli for these two end-member cases. We observe that the major control on the efficiency is the volume of intrusion emplaced rather than the crystallinity of the mush prior to melting. The efficiency, although time dependent and monotonically decreasing after a short amount of time (less than a year from our calculations), remains substantially greater than 1 for most cases.

5. Discussion

5.1. Mechanical self-assimilation

The non-linear interaction between (1) melting, which affects the proportions of the three phases as well as the mobility of the fluid phases, (2) the mass transfer of volatiles and (3) the pressure evolution of the system, which affects the density and saturation of the volatile phase (hence their mobility), makes an intuitive prediction of the evolution of a mush during its rejuvenation particularly challenging. In this section, we attempt to extract a better understanding of the results we obtained from the numerical experiments.

As observed from Eq. (19), the ability of the reactivated fraction of the mush to build up some overpressure depends on many factors. The two first factors are the source terms for the pressure increase, the

Please cite this article as: Huber, C., et al., Thermo-mechanical reactivation of locked crystal mushes: Melting-induced internal fracturing and assimilation processes in magmas, Earth Planet. Sci. Lett. (2011), doi:10.1016/j.epsl.2011.02.022

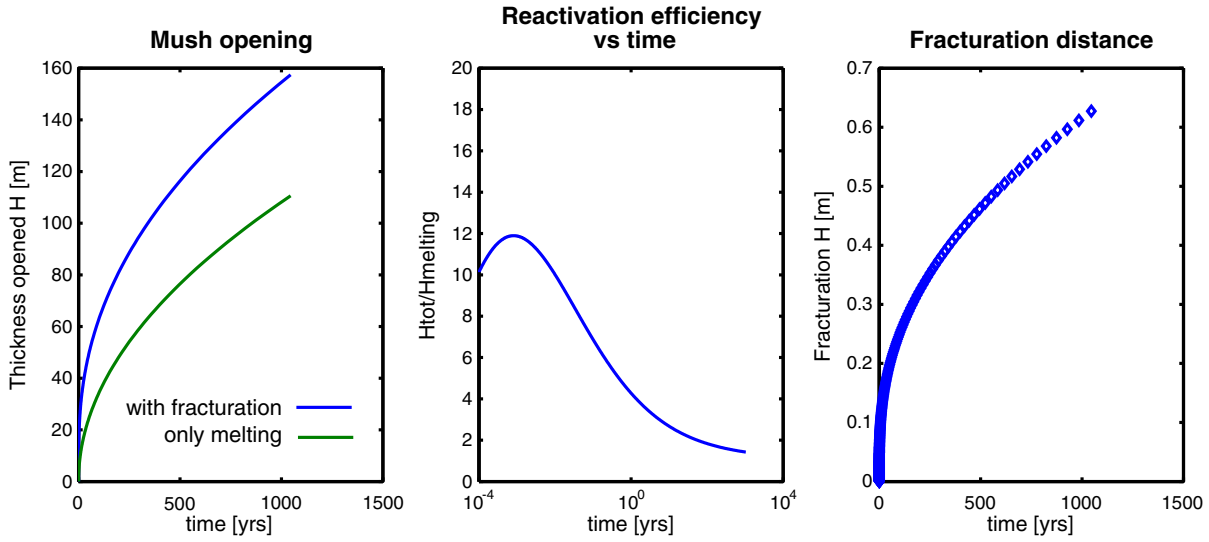

Fig. 6. Results obtained for a mush initially with 67% crystals, an intrusion–mush volume ratio of 1/2 and a host-rock bulk modulus of 10^{11} Pa. (a) shows a comparison between the temporal evolution of the position of the melting front with and without fracturing. (b) shows the evolution of $\zeta(t)$, see Eq. (31). (c) shows the penetration distance of each fracturing episode calculated with Eq. (29).

solid–liquid phase change associated with melting and the injection of volatiles from the intrusion. The results of our numerical calculations point strongly to melting as the main source for the pressure increase (tested by removing sequentially each term of the right hand side of Eq. (19)). The more subtle effect of the injection of volatiles can be explained with the following argument. As the volatile content (and

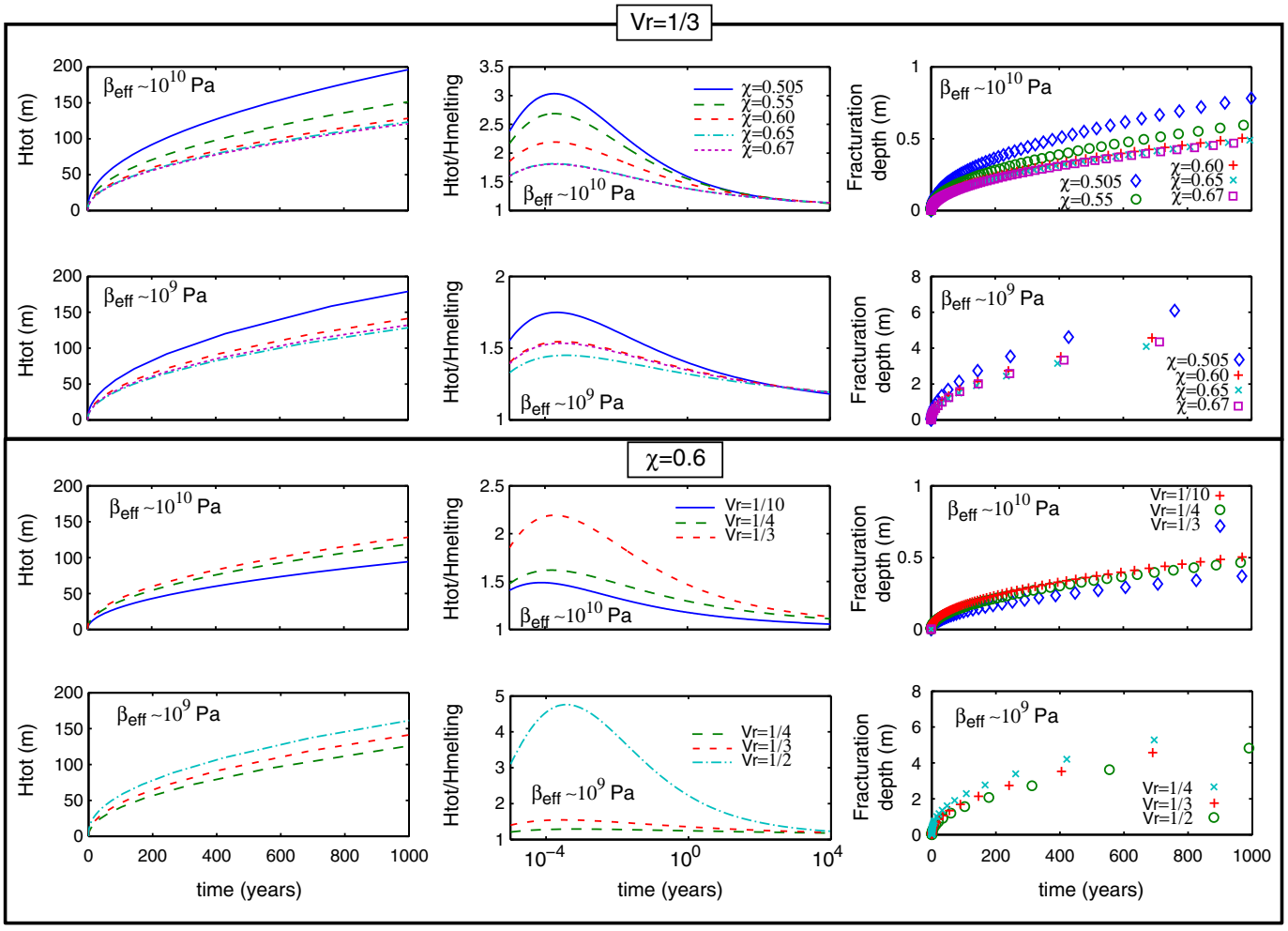

Fig. 7. Examples of results obtained for the temporal reactivation of crystal mushes. The first two rows show calculations conducted for a fixed intrusion–mush volume ratio of 1/3 and the last two rows for a fixed initial mush crystallinity of 0.6.

Please cite this article as: Huber, C., et al., Thermo-mechanical reactivation of locked crystal mushes: Melting-induced internal fracturing and assimilation processes in magmas, Earth Planet. Sci. Lett. (2011), doi:10.1016/j.epsl.2011.02.022

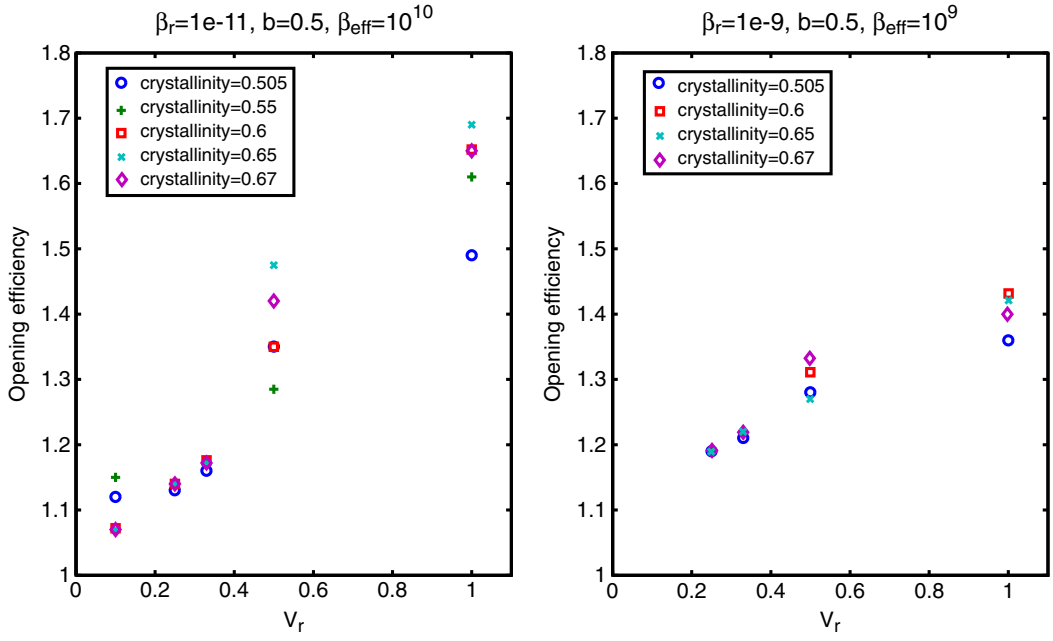

Fig. 8. Opening efficiencies (ζ) as function of intrusion–mush volume ratio V_r and initial mush crystallinity for two different end-members for the host-rock bulk modulus β_r and a power–law exponent in Eq. (7) set to 0.5. (a) shows a case where the host-rocks behave rigidly and (b) a case where thermal or mechanical effects associated with the emplacement of the magma made the host-rocks much weaker. The effect of β_{eff} is associated with a decrease of the slope of the efficiency–Vr relationship by half from left to right.

therefore the total mass) in the mush increases, the effective bulk modulus, more specifically the Hashin–Shtrikman–Walpole bounds (Eq. (18)) for the bulk modulus of the mixture, decreases. In other words, the injected volatile phase increase the compressibility of the magma mixture and the pressure build-up becomes less efficient.

Another important factor tested during our numerical calculations is the host-rock bulk modulus. One can imagine two endmember cases, (1) where the host-rock are strong and not affected by the magmatic system (we chose $\beta r = 10^{11}$ Pa), and, (2)a case where the host-rocks are significantly weaker because of the heat of the intrusion–mush system as well as possibly some mechanical weakening associated with the emplacement of magma ($\beta r = 10^{9}$ Pa). The last variable we tested that can have a significant impact on the mush behavior is the volume of the injection (again assumed to be emplaced at once for simplicity), or similarly the volume ratio V_r between the intrusion and the mush.

Our results suggest that the volume ratio of intrusion to mush V_r exerts the main control on the efficiency of fracturing episodes to assist the reactivation of the mush. The importance of the volume of intrusion lies in the fact that a more voluminous andesitic intrusion (given a certain emplacement temperature) provides more enthalpy to the mush. It also allows the intrusion to remain at a greater temperature (closer to the emplacement temperature) for a longer time. The heat flux from the intrusion to the mush remains important for a longer duration than for smaller intrusions. A secondary positive effect is that a greater intrusion with the same initial weight fraction of dissolved volatiles is expected to be able to exsolve (by secondary boiling) and transfer more volatiles to the mush over the course of its cooling. However, the cooling rate being smaller for larger intrusions, the transfer of volatiles from the intrusion to the mush is expected to take more time.

The crystallinity of the mush prior to the reactivation χ_{ini} plays a more complicated role in the reactivation of the mush. After a reactivation event of about a thousand years, it appears that the initial crystallinity is not an important factor in terms of the fracturing efficiency. One has to remember, however, that the definition of ζ here points to the relative effect of fracturing episodes on the reactivation. In absolute value, a mush with a greater initial crystallinity requires a greater input of enthalpy to be rejuvenated. The absolute volume of mush reactivated is therefore strongly controlled by χ_{ini}. The effect of the self-assimilation then appears to be similar for various χ_{ini}, however the likelihood of the mush being reactivated is much greater for values of χ_{ini} closer to the rheological transition.

Various tests illustrate that the value of the bulk modulus of the host rocks β_r and of the multiphase magmatic mixture in the reactivated part of the mush $\beta_{HS}^{(3)}$, or together as β_{eff} has a significant influence on both the frequency of fracturing episodes and on the volume of mush assimilated during each of these episodes. Focusing on the dominant term of Eq. (19) for the build-up of overpressure, we can use a simple argument to show that the fracturing period $\mathcal{T} \sim t^{\mathcal{C}}$ where $\mathcal{C} \sim 1$.

$$\frac{dp}{dt} \sim \frac{\Delta\rho}{\overline{\rho}} \beta_{\text{eff}} \frac{d\overline{\phi}}{dt}. \tag{32}$$

The period $\mathcal{T}$ can be obtained by rearranging the previous equation

$$\mathcal{T} \sim \Delta p \left(\frac{\Delta\rho}{\overline{\rho}} \beta_{\text{eff}} \frac{d\overline{\phi}}{dt} \right)^{-1}, \tag{33}$$

where Δp is again the overpressure required for fracturing (here 10^7 Pa). Assuming for simplicity that $\overline{\rho}$ and β_{eff} remains roughly constant during the reactivation (the difference in density and bulk modulus between the melt and solid phase is not too large), the only time-dependent term is $d\overline{\phi} / dt$

$$\frac{d\overline{\phi}}{dt} = \frac{1}{H(t)} \int_0^{H(t)} \frac{\partial \phi}{\partial t} dz, \tag{34}$$

where $H(t)$ is the thickness of mush remobilized. Due to small $H(t)$, we neglect heat transfer due to the expected sluggish convection

$$\frac{\partial \phi}{\partial t} \sim c(\text{St}) \sqrt{\frac{\kappa_{\text{mix}}}{t}}, \tag{35}$$

where κ_{mix} is the multiphase average thermal diffusivity of the magma. The coefficient $c(\text{St})$ depends on the Stefan number $\text{St} = c(T_{\text{intr}} - T_{\text{lock}})/L_f$, where c is the multiphase average specific heat of the magma, L_f the

Please cite this article as: Huber, C., et al., Thermo-mechanical reactivation of locked crystal mushes: Melting-induced internal fracturing and assimilation processes in magmas, Earth Planet. Sci. Lett. (2011), doi:10.1016/j.epsl.2011.02.022

latent heat associated with melting and T_{lock} is the temperature at the mush reactivation front. Assuming that the bulk of the melting occurs over a narrow region of roughly constant thickness at the interface between the reactivated and locked parts of the mush,

$$\frac{d\overline{\phi}}{dt} \sim \frac{c(\mathrm{St})}{H(t)}\sqrt{\frac{\kappa_{\mathrm{mix}}}{t}}. \tag{36}$$

The thickness of reactivated mush, with our simplifying assumption that the heat transfer is mostly diffusive also depends on time

$$H(t) \sim c(\mathrm{St})\sqrt{\kappa_{\mathrm{mix}} t}. \tag{37}$$

According to this simple scaling argument, the period between fracturing events becomes

$$\mathcal{T} \sim \frac{\overline{\rho}\Delta p}{\Delta\rho\beta_{eff}} t. \tag{38}$$

The prefactor for the time-dependence of the period between consecutive fracturation episodes $\overline{\rho}\Delta p / (\Delta\rho\beta_{\mathrm{eff}}) \sim 0.01$, which is in good agreement with the slope of 0.036 found in Fig. 4a. We note that assuming that the heat transfer is mostly advective leads also to a linear relationship between the period of fracturing and time. Indeed, assuming that the advective heat flux is roughly constant over time, gives $\partial\phi/\partial t \sim$ constant and $H(t) \sim t$. This scaling argument predicts a linear relationship between the period between consecutive fracturing episodes and time, however, it basically assumed that the temperature at the interface between the mush and the intrusion remains constant over time. For a cooling intrusion, one should expect the efficiency of melting to decrease with time and therefore that the power law exponent is more realistically >1. We found power–law exponents ranging between 1.1 and 1.25 with our numerical calculations.

We showed that the solid–liquid phase transition dominates the pressure evolution in the mush during its reactivation, provided there is a sufficient difference in density between the two phases. Similarly, while the intrusion cools and crystallizes, one should expect the pressure in the intrusion to decrease. A pressure decrease in the underlying intrusion could partially absorb the overpressure in the mush and decrease the fracturing efficiency. The crystallization of the intrusion induces however two opposing effects. First, it is responsible for the exsolution of volatiles, which buffer the pressure evolution in the intrusion (Huppert and Woods, 2002). Second, a mushy boundary layer between the intrusion and the mush will grow at the contact with the cooler mush, and, as observed from the pressure diffusion profile above the melting front in our calculations (Fig. 3d), the diffusion of the overpressure in the mush is fairly inefficient. Table 2 summarizes the effect of these different variables in the scope of the efficiency of the mechanical self-assimilation mechanism for the reactivation of crystal mushes.

5.2. Mechanical bulk assimilation

In a vast number of magmatic provinces around the world, fractional crystallization coupled with some country rock assimilation (AFC) is referred to as the dominant process by which magmas diversify (laid out in the scientific literature at least since (Bowen, 1928; Daly, 1914)). Although this process is well characterized chemically (obvious correlations between different isotopic systems; e.g., (Taylor, 1980), presence of xenocrysts, particularly obvious when they can be dated; e.g., among many (Bindeman et al., 2008; Lanphere and Baadsgaard, 2001; Schmitt et al., 2003; Vazquez and Reid, 2002) or isolated chemically; (Charlier et al., 2007)), the physical processes at the origin of this assimilation remain controversial (Beard et al., 2004; Beard et al., 2005; Clarke and Erdmann, 2008; Glazner and Bartley, 2006; Glazner and Bartley, 2008; Paterson et al., 2008; Spera and Bohrson, 2004; Yoshinobu and Barnes, 2008; Yoshinobu et al., 2003).

There are two end member processes by which assimilation can occur in magmas: (1) assimilation by partially melting the wall-rocks and incorporation of the partial melt in the differentiating magma (e.g., Spera and Bohrson, 2004), and (2) bulk assimilation (whole blocks of crust being incorporated into the magma, generally, but not necessarily, by a mechanism refer to as stoping after the practice of working the roofs of underground mines). Although melt assimilation is still considered as a potentially important process in the crust and used in AFC models (Bohrson and Spera, 2007; Glazner and Bartley, 2006), multiple lines of evidence suggest that bulk assimilation is geologically, mechanically and energetically more likely (Beard et al., 2005; Yoshinobu and Barnes, 2008), at least in the upper crust. As shown in this paper, the melting process that necessarily occurs when fusible blocks of solidified crust enter in contact with hotter magmas will aid the disaggregation of wall rock pieces into small xenoliths or xenocrysts. This reduction in grain size will allow efficient peritectic reactions to take place, leading to the texturally cryptic assimilation presented by (Beard et al., 2005). This bulk assimilation process differs from self-assimilation as the assimilated mass is related to pre-existing wall rocks that were once fully crystallized (and not earlier co-genetic magma intrusions that may have never gone below their solidii). However, mechanically, those two processes are equivalent (in both processes, melting and fracturation lead to breaking and dispersion of assimilated material).

6. Conclusions

The mechanical weakening of the locked-up mush in response to melting and gas addition (loss of strength and build up of overpressure) offers a plausible hypothesis to explain the observation of large reactivated crystal mushes that erupt with average crystallinities higher than 40 vol%. As shown by (Huber et al., 2010b), melting models alone prove to be (1) unable to explain the high average crystallinity of for example Monotonous Intermediates and also (2) require unrealistic volumes of intrusion for the reactivation of large crystal-rich magma bodies. The mechanical self-assimilation mechanism proposed here potentially alleviates these two problems. Each fracturing event allows for a mixing between the magma in the already reactivated part of the mush with the assimilate (crystallinity similar to the mush). These repeated episodes lead to a greater crystallinity than expected from melting alone in the rejuvenated mush. Moreover, the self-assimilation mechanism is triggered by the overpressure build-up by melting and therefore does not require more energy than what is already accounted for in the case of a thermal reactivation by melting. Our calculations reveal that, in some cases, the volume of mush reactivated for a given thermal energy input can be increased substantially (about 1000% at early times and about 60% after 1000 years). Although not discussed here, the effect of smaller but repeated intrusions is expected to increase the efficiency

Table 2
Summary of the coupling between the different processes and their effect on the reactivation efficiency ζ.

Factor	Effect	Correlation with efficiency
V_r	Enthalpy injected, heat flux versus time	+
β_r	"Rigidity of the container"	+ for Δp; − for ΔV_{frac}, − overall
Volatile flux from intrusion	Increase mass, decrease β_{eff}	+, Δp>0 but ↘ with S_g↗
Melting	Increase Δp, phase change	+

Please cite this article as: Huber, C., et al., Thermo-mechanical reactivation of locked crystal mushes: Melting-induced internal fracturing and assimilation processes in magmas, Earth Planet. Sci. Lett. (2011), doi:10.1016/j.epsl.2011.02.022

of the self-assimilation process by sustaining the heat flux from the intrusion to the mush to greater values for longer durations.

Similar processes of overpressure build-up during the partial melting of country rocks are also expected to play an important role in facilitating bulk assimilation processes. In this particular case, melting both weakens the country rock in contact with a magmatic intrusion and also provides some mechanical work to disaggregate blocks (approximately to the cm scale) which can be further downsized by bulk assimilation processes.

Acknowledgement

The authors would like to thank the editor R. Carlson, an anonymous reviewer and J. Beard for their useful comments and suggestions. C.H. was funded by a Swiss postdoctoral fellowship, O.B. acknowledges funding from NSF-EAR 0809828 and J.D. from NSF-EAR 0948352.

References

Assael, M.J., Bekou, E., Giakoumakis, D., Friend, D.G., Killeen, M.A., Millat, J., 2000. Experimental data for the viscosity and thermal conductivity of water and steam. J. Phys. Chem. 141, 1.556056 Ref. Data.

Bachmann, O., Dungan, M.A., Lipman, P.W., 2002. The Fish Canyon magma body, San Juan volcanic field, Colorado: rejuvenation and eruption of an upper crustal batholith. J. Petrol. 43, 1469–1503.

Bachmann, O., Charlier, B.L.A., Lowenstern, J.B., G.W., 2007. Zircon crystallization and recycling in the magma chamber of the rhyolitic Kos Plateau Tuff (Aegean arc), 35, pp. 73–76.

Bear, J., 1988. Dynamics of Fluids in Porous Media. Dover, p. 784.

Beard, J.S., Ragland, P.C., Crawford, M.L., 2005. Reactive bulk assimilation: a model for crust–mantle mixing in silicic magmas. Geology 33 (8), 681–684.

Beard, J.S., Ragland, P.C., Rushmer, T., 2004. Hydration crystallization reactions between anhydrous minerals and hydrous melt to yield amphibole and biotite in igneous rocks: description and implications. J. Geol. 112, 617–621.

Bindeman, I.N., Fu, B., Kita, N.T., Valley, J.W., 2008. Origin and evolution of silicic magmatism at Yellowstone based on ion microprobe analysis of isotopically zoned zircons. J. Petrol. 49 (1), 163–193.

Bohrson, W.A., Spera, F.J., 2007. Energy-constrained recharge, assimilation, and fractional crystallization (EC-RAFC): a visual basic computer code for calculating trace element and isotope variations of open-system magmatic systems. Geochem. Geophys. Geosyst. 8.

Bowen, N.L., 1928. The Evolution of Igneous Rocks. Dover publications, New York, p. 332.

Charlier, B.L.A., Bachmann, O., Davidson, J.P., Dungan, M.A., Morgan, D., 2007. The upper crustal evolution of a large silicic magma body: evidence from crystal-scale Rb/Sr isotopic heterogeneities in the Fish Canyon magmatic system, Colorado. Journal of Petrology 48 (10), 1875–1894 (very large volume ignimbrites: Geol. Mag., v. 6, p. 669-681.).

Clarke, D.B., Erdmann, S., 2008. Is stoping a volumetrically significant pluton emplacement process?: Comment. Geol. Soc. Am. Bull. 120 (7–8), 1072–1074.

Couch, S., Sparks, R.S.J., Carroll, M.R., 2001. Mineral disequilibrium in lavas explained by convective self-mixing in open magma chambers. Nature 411, 1037–1039.

Daly, R.A., 1914. Igneous Rocks and Their Origin. McGraw-Hill, London, p. 563. vol.

Daly, R.A., 1933. Igneous Rocks and the Depths of the Earth. McGraw Hill, New York. vol.

DePaolo, D.J., 1981. Trace element and isotopic effects of combined wallrock assimilation and fractional crystallization. Earth Planet. Sci. Lett. 53, 189–202.

Dufek, J., Bergantz, G.W., 2005. Lower crustal magma genesis and preservation: a stochastic framework for the evaluation of basalt–crust interaction. J. Petrol. 46, 2167–2195.

Glazner, A.F., Bartley, J.M., 2006. Is stoping a volumetrically significant pluton emplacement process? Geol. Soc. Am. Bull. 118 (9–10), 1185–1195.

Glazner, A.F., Bartley, J.M., 2008. Reply to comments on âIs stoping a volumetrically significant pluton emplacement process? Geol. Soc. Am. Bull. 120 (7–8), 1082–1087.

Ghiorso, M.S., Sack, R.O., 1995. Chemical mass transfer in magmatic processes IV: a revised and internally consistent thermodynamic model for the interpolation and extrapolation of liquid–solid equilibria in magmatic systems at elevated temperatures and pressures. Contrib. Mineralog. Petrol. 119, 197–212.

Halbach, H., Chatterjee, N.D., 1982. An empirical Redlich–Kwong equation of state for water to 1000 °C and 200 kbar. Contrib. Mineralog. Petrol. 79, 337–345.

Hashin, Z., Shtrikman, S., 1963. A variational approach to the theory of elastic behavior of multiphase materials. J. Mech. Phys. Solids 11, 127–140.

Hildreth, W., 1981. Gradients in silicic magma chambers: implications for lithospheric magmatism. J. Geophys. Res. 86, 10153–10192.

Huber, C., Bachmann, O., Manga, M., 2010a. Two competing effects of volatiles on heat transfer in crystal-rich magmas: thermal insulation vs defrosting. J. Petrol. 51, 847–867.

Huber, C., Bachmann, O., Dufek, J., 2010b. The limitations of melting in the rejuvenation of silicic crystal mushes. J. Volcanol. Geoth. Res. 195, 97–105.

Huppert, H.E., Woods, A.W., 2002. The role of volatiles in magma chamber dynamics. Nature 420, 493–495.

Karlstrom, L., Dufek, J., Manga, M., 2010. Magma chamber stability in arc and continental crust. J. Volcanol. Geoth. Res. 190, 249–270.

Koyaguchi, T., Kaneko, K., 2001. Thermal evolution of silicic magma chambers after basalt replenishment. Trans. R. Soc. Edimburgh 91, 47–60.

Lanphere, M.A., Baadsgaard, H., 2001. Precise K–Ar, 40Ar/39Ar, Rb–Sr, U/Pb mineral ages from the 27.5 Ma Fish Canyon Tuff reference standard. Chem. Geol. 175, 653–671.

Lemmon, E.W., McLinden, M.O., Friend, D.G., 2003. Thermophysical properties of fluid systems. NIST Chemistry WebBook, NIST Standard Reference Database, 69.

Mahood, G.A., 1990. A second reply to "Comment by R.S.J. Sparks, H.E. Huppert, and C.J. N. Wilson on "Evidence for long residence times of rhyolitic magma in the Long Valley magmatic system: the isotopic record in theprecaldera lavas of Glass Mountain"". Earth Planet. Sci. Lett. 99, 395–399.

Menand, T., Tait, S.R., 2001. A phenomenological model for precursor volcanic eruptions. Nature 411, 678–680.

Murphy, M.D., Sparks, R.S.J., Barclay, J., Carroll, M.R., Brewer, T.S., 2000. Remobilization of andesite magma by intrusion of mafic magma at the Soufriere Hills volcano, Montserrat, West Indies. J. Petrol. 41, 21–42.

Nakamura, M., 1995. Continuous mixing of crystal mush and replenished magma in the ongoing Unzen eruptionm. Geology 23, 807–810.

Pallister, J.S., Hoblitt, R.P., Reyes, A.G., 1992. A basalt trigger for the 1991 eruptions of Pinatubo volcano? Nature 356, 426–428.

Parat, F., Holtz, F., Feig, S., 2008. Pre-eruptive conditions of the Huerto Andesite (Fish Canyon System, San Juan Volcanic Field, Colorado): influence of volatiles (C–O–H–S) on phase equilibria and mineral composition. J. Petrol. 49 (5), 911–935.

Paterson, S.R., Pignotta, G.S., Farris, D., Memetti, V., Miller, R.B., Vernon, R.H., 2008. Is stoping a volumetrically significant pluton emplacement process?: Discussion. Geol. Soc. Am. Bull. 120 (7–8), 1075–1079.

Paterson, S.R., Janousek, V., 2008. Growth of complex sheeted zones during recycling of older magmatic units into younger: Sawmill Canyon area, Tuolumne batholith, Sierra Nevada, California. J. Volcanol. Geoth. Res. 177 (2), 457–484.

Robinson, D.M., Miller, C.F., 1999. Record of magma chamber processes preserved in accessory mineral assemblages, Aztec Wash pluton, Nevada. Am. Mineralog. 84, 1346–1353.

Rubin, A.M., 1998. Dike ascent in partially molten rock. J. Geophys. Res. 103 (B9), 20,901–20, 919.

Snyder, D., 2000. Thermal effects of the intrusion of basaltic magma into a more silicic magma chamber and implications for eruption triggering. Earth Planet. Sci. Lett. 175, 257–273.

Schmitt, A.K., Lindsay, J.M., de Silva, S., Trumbull, R.B., 2003. IU–Pb zircon chronostratigraphy of early-Pliocene ignimbrites from La Pacana, north Chile: implications for the formation of stratified magma chambers. J. Volcanol. Geoth. Res. 120 (1–2), 43–53.

Spera, F.J., Bohrson, W.A., 2004. Open-system magma chamber evolution: an energy-constrained geochemical model incorporating the effects of concurrent eruption, recharge, variable assimilation and fractional crystallization (EC-E'RAchiFC). J. Petrol. 45 (12), 2459–2480.

Taylor, H.P., 1980. The effects of assimilation of country rocks by magmas on 18O/16O and 87Sr/86Sr systematics in igneous rocks. Earth Planet. Sci. Lett. 47, 243–254.

Torquato, S., 2001. Random Heterogeneous Materials. Springer, p. 728.

Vazquez, J.A., Reid, M.R., 2002. Time scales of magma storage and differentiation of voluminous high-silica rhyolites at Yellowstone caldera, Wyoming. Contrib. Mineralog. Petrol. 144 (3), 274–285.

Wiebe, R., Wark, D., Hawkins, D., 2007. Insights from quartz cathodoluminescence zoning into crystallization of the Vinalhaven granite, coastal Maine. Contrib. Mineralog. Petrol. 154 (4), 439–453.

Yoshinobu, A.S., Fowler, T.K., Paterson, S.R., Llambias, E., Tickyj, H., Sato, A.M., 2003. A view from the roof: magmatic stoping in the shallow crust, Chita pluton, Argentina. J. Struct. Geol. 25, 1037–1048.

Yoshinobu, A.S., Barnes, C.G., 2008. Is stoping a volumetrically significant pluton emplacement process?: Discussion. Geol. Soc. Am. Bull. 120 (7–8), 1080–1081.

Please cite this article as: Huber, C., et al., Thermo-mechanical reactivation of locked crystal mushes: Melting-induced internal fracturing and assimilation processes in magmas, Earth Planet. Sci. Lett. (2011), doi:10.1016/j.epsl.2011.02.022